5674 *Chem. Mater.* **2009,** *21,* 5674–5680
DOI:10.1021/cm902182y

CHEMISTRY OF MATERIALS
Article

Electrical and Spectroscopic Characterizations of Ultra-Large Reduced Graphene Oxide Monolayers

Ching-Yuan Su,[†,‡,#] Yanping Xu,[†,#] Wenjing Zhang,[†] Jianwen Zhao,[†] Xiaohong Tang,[§] Chuen-Horng Tsai,[‡] and Lain-Jong Li*[,†]

[†]*School of Materials Science and Engineering, Nanyang Technological University 50, Nanyang Avenue, 637819 Singapore,* [‡]*Department of Engineering and System Science, National Tsing Hua University, 101, section 2 Kuang Fu Road, Hsinchu 300, Taiwan, and* [§]*Photonics Research Centre, Microelectronics Division, School of Electrical and Electronic Engineering, Nanyang Technological University, 639798 Singapore.* [#] *These authors contributed equally.*

Received July 17, 2009. Revised Manuscript Received October 26, 2009

Ultra large and single-layer graphene oxide sheets (up to millimeter in lateral size) are obtained by a modified Hummers' method, where we replace the first aggressive oxidation process with a short sonication step in H_2SO_4 solutions. The lateral size of obtained GO sheets can be adjusted by the sonication period: it decreases with the increasing sonication time. The thin-film electrodes made from ultra large reduced GO sheets exhibit lower sheet resistance compared with those from small-size reduced GO sheets. Moreover, the transistor devices made from these single-layer GO sheets after 800 °C thermal reduction exhibit the effective hole mobility ranged between 4 and 12 $cm^2/(V\ s)$. Raman spectroscopic results suggest that the enhancement in mobility at a higher-mobility regime is well explained by the graphitization of GO rather than the removal of functional groups. The ratio between the 2D and G peak areas, $I(2D)/I(G)$, is well correlated to the effective hole mobility values in reduced GO sheets.

Introduction

Since the discovery of single-layer graphene (SLG),[1−3] it has attracted intensive interest because of its two-dimensionality and unique physical properties such as high intrinsic carrier mobility (∼200 000 $cm^2/(V\ s)$),[4] quantum electronic transport,[5] tunable band gap,[6,7] high mechanical strength and elasticity,[8] and superior thermal conductivity.[9] These outstanding properties make graphene promising for high speed transistor applications,[10−14] transparent conductive thin films,[14−16] reinforced composites,[17,18] and energy storage.[19] In addition to mechanical exfoliation,[1] epitaxial growth,[20−22] and chemical vapor deposition (CVD),[23,24] graphene oxide

*Corresponding author. E-mail: ljli@ntu.edu.sg.

(1) Novoselov, K. S.; Geim, A. K.; Morozov, S. V.; Jiang, D.; Zhang, Y.; Dubonos, S. V.; Grigorieva, I. V.; Firsov, A. A. *Science* **2004**, *306*, 666–669.
(2) Novoselov, K. S.; Geim, A. K.; Morozov, S. V.; Jiang, D.; Katsnelson, M. I.; Grigorieva, I. V.; Dubonos, S. V.; Firsov, A. A. *Nature* **2005**, *438*, 197–200.
(3) Novoselov, K. S.; Jiang, D.; Schedin, F.; Booth, T. J.; Khotkevich, V. V.; Morozov, S. V.; Geim, A. K.; Rice, T. M. *Proc. Natl. Acad. Sci. U.S.A.* **2005**, *102*, 10451–10453.
(4) Bolotin, K. I.; Sikes, K. J.; Jiang, Z.; Klima, M.; Fundenberg, G.; Hone, J.; Kim, P.; Stormer, H. L. *Solid State Commun.* **2008**, *146*, 351–355.
(5) Zhang, Y. B.; Tan, Y. W.; Stormer, H. L.; Kim, P. *Nature* **2005**, *438*, 201–204.
(6) Han, M. Y.; Ozyilmaz, B.; Zhang, Y. B.; Kim, P. *Phys. Rev. Lett.* **2007**, *98*, 206805.
(7) Zhang, Y. B.; Tang, T. T.; Girit, C.; Hao, Z.; Martin, M. C.; Zettl, A.; Crommie, M. F.; Shen, Y. R.; Wang, F. *Nature* **2009**, *459*, 820–823.
(8) Lee, C.; Wei, X. D.; Kysar, J. W.; Hone, J. *Science* **2008**, *321*, 385–388.
(9) Balandin, A. A.; Ghosh, S.; Bao, W. Z.; Calizo, I.; Teweldebrhan, D.; Miao, F.; Lau, C. N. *Nano Lett.* **2008**, *8*, 902–907.
(10) Chen, Z. H.; Lin, Y. M.; Rooks, M. J.; Avouris, P. "Graphene nano-ribbon electronics. In *Proceedings of the 2nd International Symposium on Nanometer-Scale Quantum Physics*; Tokyo, Jan 24−26, 2007; Tokyo Tech Physics COE21: Tokyo, 2007.
(11) Lemme, M. C.; Echtermeyer, T. J.; Baus, M.; Kurz, H. *IEEE Electron Device Lett.* **2007**, *28*, 282–284.
(12) Martin, J.; Akerman, N.; Ulbricht, G.; Lohmann, T.; Smet, J. H.; von Klitzing, K.; Yacoby, A. *Nat. Phys.* **2008**, *4*, 144–148.
(13) Das, A.; Pisana, S.; Chakraborty, B.; Piscanec, S.; Saha, S. K.; Waghmare, U. V.; Novoselov, K. S.; Krishnamurthy, H. R.; Geim, A. K.; Ferrari, A. C.; Sood, A. K. *Nat. Nanotechnol.* **2008**, *3*, 210–215.
(14) Eda, G.; Fanchini, G.; Chhowalla, M. *Nat. Nanotechnol.* **2008**, *3*, 270–274.
(15) Tung, V. C.; Chen, L. M.; Allen, M. J.; Wassei, J. K.; Nelson, K.; Kaner, R. B.; Yang, Y. *Nano Lett.* **2009**, *9*, 1949–1955.
(16) Becerril, H. A.; Mao, J.; Liu, Z.; Stoltenberg, R. M.; Bao, Z.; Chen, Y. *ACS Nano* **2008**, *2*, 463–470.
(17) Stankovich, S.; Dikin, D. A.; Dommett, G. H. B.; Kohlhaas, K. M.; Zimney, E. J.; Stach, E. A.; Piner, R. D.; Nguyen, S. T.; Ruoff, R. S. *Nature* **2006**, *442*, 282–286.
(18) Xie, S. H.; Liu, Y. Y.; Li, J. Y. *Appl. Phys. Lett.* **2008**, *92*, 243121.
(19) Yoo, E.; Kim, J.; Hosono, E.; Zhou, H.; Kudo, T.; Honma, I. *Nano Lett.* **2008**, *8*, 2277–2282.
(20) Berger, C.; Song, Z. M.; Li, X. B.; Wu, X. S.; Brown, N.; Naud, C.; Mayou, D.; Li, T. B.; Hass, J.; Marchenkov, A. N.; Conrad, E. H.; First, P. N.; de Heer, W. A. *Science* **2006**, *312*, 1191–1196.
(21) Sutter, P. W.; Flege, J. I.; Sutter, E. A. *Nat. Mater.* **2008**, *7*, 406–411.
(22) Liang, X.; Fu, Z.; Chou, S. Y. *Nano Lett.* **2007**, *7*, 3840–3844.
(23) Reina, A.; Jia, X. T.; Ho, J.; Nezich, D.; Son, H.; Bulovic, V.; Dresselhaus, M. S.; Kong, J. *Nano Lett.* **2009**, *9*, 30–35.
(24) Li, X. S.; Cai, W. W.; An, J. H.; Kim, S.; Nah, J.; Yang, D. X.; Piner, R.; Velamakanni, A.; Jung, I.; Tutuc, E.; Banerjee, S. K.; Colombo, L.; Ruoff, R. S. *Science* **2009**, *324*, 1312–1314.
(25) Park, S.; Ruoff, R. S. *Nat. Nanotechnol.* **2009**, *4*, 217–224.
(26) Park, S.; An, J. H.; Jung, I. W.; Piner, R. D.; An, S. J.; Li, X. S.; Velamakanni, A.; Ruoff, R. S. *Nano Lett.* **2009**, *9*, 1593–1597.
(27) Stankovich, S.; Dikin, D. A.; Piner, R. D.; Kohlhaas, K. A.; Kleinhammes, A.; Jia, Y.; Wu, Y.; Nguyen, S. T.; Ruoff, R. S. *Carbon* **2007**, *45*, 1558–1565.

Published on Web 11/11/2009

(GO) has been recently considered as potential carbon-based nanomaterials for producing graphene[14,25−28] The exfoliated single-layer GO sheets can be well dispersed in aqueous solutions, which provides a solution and low temperature process to make single-layer graphene sheets. Also, the solution-compatible process is potential in large-area, scalable and flexible electronics. According to the commonly used Hummers' method,[29] graphite powders were treated with oxidation for adding oxygen-containing functional groups on the edges and the basal planes of graphite flakes. These decorated functional groups were able to reduce the interplanar forces and promote complete exfoliation of single-layer GO sheets in aqueous media. However, the size of as-prepared GO sheets in most reports ranges from 100 nm to several micrometers,[25] which may hinder the development toward practical applications, especially in large area conductive thin films. Recently, Luo et al. have obtained large size single-layer GO sheets (up to 2000 μm^2 in size) by involving pre-exfoliation of the graphite by microwave heating,[28] which provides a hint that additional oxidation process help to exfoliate layers of graphite flakes. On the other hand, to obtain graphene sheets GO has to be converted back to conducting graphene (reduced GO) through removal of the oxygen-containing functional groups (e.g., C═O and C−OH). Two main approaches have been reported to obtain reduced GO: (1) exposed to hydrazine vapor,[14,25−28] and (2) thermal annealing.[14,16,17,28] In a recent study,[16] the thermal reduction method has been demonstrated to be the most effective treatment in deoxygenating and restoring conductivity. However, the relation between degree of graphitization and carrier mobility in single-layer reduced GO are still unclear. Cristina et al. demonstrated for the first time that the hole mobility of the GO sheets after the exposure to hydrazine vapor and hydrogen plasma, is around 0.001−1 $cm^2/(V\ s)$.[30]

In this contribution, we introduce a sonication process to Hummers' method and we find that the lateral size of obtained GO sheets can be better adjusted by the sonication period. The modified process allows us to exfoliate ultralarge single-layer GO sheets from graphite flakes, up to several square millimeter in size. The thin-film electrodes made from ultralarge reduced GO sheets exhibit lower resistance compared with those from small-size reduced GO sheets. The transistor devices made from these single-layer GO after 800 °C thermal reduction exhibit the effective field effect hole mobility from 4 to 12 $cm^2/(V\ s)$. The obtained large reduced GO sheets allow us to study their electrical properties and Raman characteristics. The enhancement in mobility after high temperature reduction is well correlated to the graphitization of GO rather than the removal of functional groups.

Experimental Section

Preparation of Large Graphene Oxide Sheets. Graphene oxide (GO) sheets were prepared by the modified Hummers' method from natural graphite flakes (average size is 3−5 mm from NGS Naturgraphit GmbH, Leinburg, Germany). We modified the Hummers' method reported by Xu et al.,[31] where we replace the first step (the chemical oxidation of graphite flakes using concentrated H_2SO_4, P_2O_5, and $K_2S_2O_8$) with a bath sonication process. And the sonication period strongly affects the size of the monolayered GO obtained. In brief, the graphite flakes (2 g) were mixed with concentrated H_2SO_4 (12 mL) and kept at 80 °C for 4.5 h. The solution was cooled to room temperature and then put into the water-bathed sonication (at 300 W) for 1−6 h in concentrated H_2SO_4, where the process helps to break the graphite into smaller and thinner flakes. The solution was then diluted with 0.5 L of deionized (DI) water and left overnight. The preoxidized graphite powders were obtained after filtration with porous filters (200 nm pore size). The product was dried in a drybox with gentle baking (70 °C). To exfoliate the graphite flakes into GO sheet, we put the preoxidized graphite powders into concentrated H_2SO_4 (120 mL), added $KMnO_4$ (15 mg), following by stirring at room temperature for 2 h. The solution was diluted with DI water (250 mL) and stirred for 2 h, and then an additional 0.7 L of DI water was added. Shortly, 20 mL of H_2O_2 (30%) was added into the mixture. After setting overnight, upper portions of the solution were colleted (unreacted graphite powders precipitated in the bottom of solution) and then centrifuged (at 10 000 rpm). The obtained powders were then dissolved in a 1:10 HCl solution and then centrifuged to remove unwanted metal ions. The powders were then dissolved in DI water and then centrifuged to remove the acid. The yield of GO sheets for the whole process was about 4.3 wt %.

Preparation of Thin-Film Electrodes. Quartz substrates (24.5 mm in diameter; 1.00 mm thick) were cleaned with a standard Piranha process. The surfaces become hydrophilic after Piranha treatment. Single-layer GO suspension was then directly air-sprayed[32] or dip-coated onto the substrates. The reduction processes (i.e., hydrazine vapor reduction and thermal annealing at elevated temperature under 20% H_2/Ar) were then applied to the GO-coated substrates. Sheet resistance was measured using a four point probe (Keithley Instrument), and the transmittance measurement was performed in a UV−vis−NIR spectrophotometer (Perkin-Elmer).

Reduction Processes and Device Fabrication. Single-layer GO films were deposited onto silicon substrates with 300 nm silicon oxide layer by the dip-coating or air-spraying method. For the hydrazine vapor reduction, samples were put into a glass bottle and 200 μL of 98% hydrazine monohydrate (Sigma) was dropped in the bottle. The samples were kept in the sealed bottle at 80 °C for 24 h. For hydrogen annealing, samples were loaded into a quartz furnace and treated at a moderate temperature (400−1000 °C in this work) for 2h under 80 sccm of hydrogen gas (20% in Ar). For the transistor device fabrication, the SLG transistor is fabricated by evaporating Au electrodes (40 nm thick) directly on top of the selected, large-size and reduced GO films using copper grid (200 mesh, 20 μm spacing) as a hard-mask, where no photoresist was used to ensure the electrical characteristics were not affected by the photoresist or other wet-chemicals necessary for the electrode patterning.

(28) Luo, Z. T.; Lu, Y.; Somers, L. A.; Johnson, A. T. C. *J. Am. Chem. Soc.* **2009**, *131*, 898.
(29) Hummers, W. S.; Offeman, R. E. *J. Am. Chem. Soc.* **1958**, *80*, 1339–1339.
(30) Gomez-Navarro, C.; Weitz, R. T.; Bittner, A. M.; Scolari, M.; Mews, A.; Burghard, M.; Kern, K. *Nano Lett.* **2009**, *9*, 5.
(31) Xu, Y. X.; Bai, H.; Lu, G. W.; Li, C.; Shi, G. Q. *J. Am. Chem. Soc.* **2008**, *130*, 5856–5857.
(32) Tantang, H.; Ong, J. Y.; Loh, C. L.; Dong, X. C.; Chen, P.; Chen, Y.; Hu, X.; Tan, L. P.; Li, L. J. *Carbon* **2009**, *47*, 1867–1870.

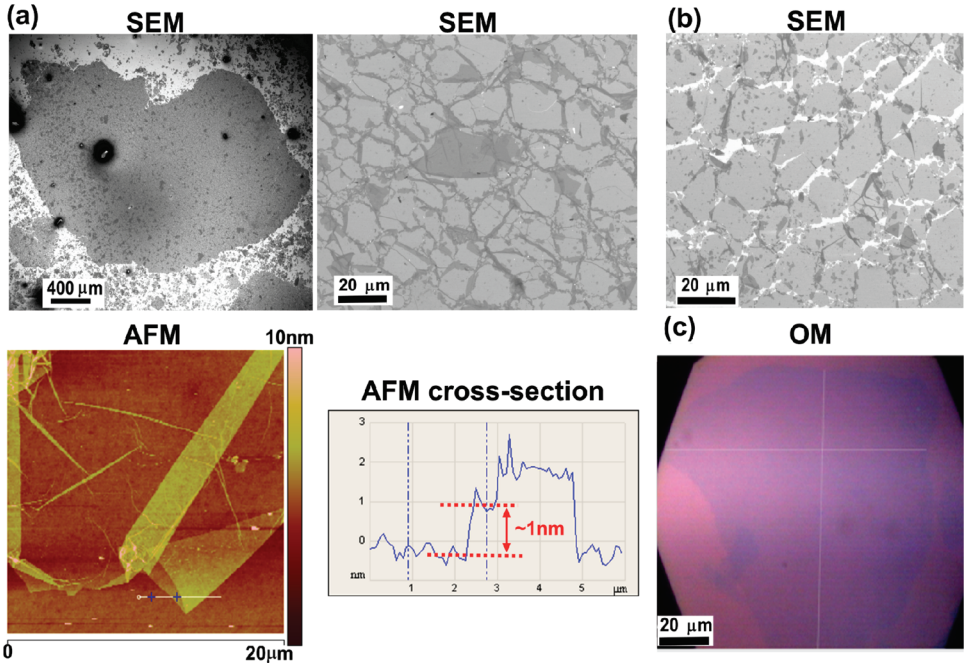

Figure 1. (a) SEM and AFM images of the ultralarge GO sheets (on quartz) produced from the modified method (with 1 h sonication). (b) SEM photo for the ultralarge single-layer GO sheet after the 800 °C reduction process. (c) The optical micrograph for the GO sheets produced from the modified method with 2 h sonication.

Characterizations and Electrical Measurements. The Raman spectra were performed in a WITec CRM200 confocal Raman microscopy system (laser wavelength 488 nm and laser spot size is ~0.5 μm) and Si peak at 520 cm^{-1} was used as a reference for wavenumber calibration. The typical channel length between source and drain electrodes is around 20 μm. All electrical measurements were performed in ambient conditions using a Keithley semiconductor parameter analyzer, model 4200-SCS.

Results and Discussions

Since 19th century, graphite oxide has been produced by Hummers' method,[14,27,29,31] which typically involves oxidation of graphite in the presence of strong oxidants and acids for extended periods. Here we modified the Hummers' method used by Xu et al.,[31] where we replace the first step (chemical oxidation of graphite flakes using strong oxidants H_2SO_4, P_2O_5, and $K_2S_2O_8$) with a sonication process in H_2SO_4 solutions to break graphite flakes into the smaller and thinner flakes. We find that the lateral size of GO monolayers obtained after the subsequent oxidation processes can be better adjusted by the sonication period, where longer sonication time results in smaller GO sheets. Interestingly, a short sonication process (1 h) allows us to obtain ultralarge GO sheets from natural graphite flakes. Figure 1a show the SEM and AFM images of the ultralarge GO sheets dip-coated on substrates. The GO sheets are up to 3 mm in lateral size, and the magnified image shows that the GO sheet has a wrinkled surface, likely unavoidable during the dip-coating process because of its ultralarge size. The AFM height profile in Figure 1a for the edge of the single GO sheet shows that the obtained GO sheet is monolayered (~1 nm). Some small GO fragments can also be found on top of the large GO sheet. The images in Figure 1a show almost perfect connection between each flat domain without exposing the underlying substrates, implying that the ultralarge GO sheet is not composed of separate GO sheets because the dip-coating method is unlikely to achieve such a well-connected GO film. We show in the Supporting Information, Figure S1, that small GO sheets (prepared with 6 h of sonication) are sparsely distributed on substrates by the same dip-coating method, in clear contrast to the ultralarge film. It is noted that small GO sheets on substrates are unlikely to achieve 100% coverage even using the Langmuir−Blodgett method to deposit the monolayered GO sheets.[33] More photographs of ultralarge and monolayered GO sheets are provided in supporting Figure S2. Figure 1b shows the SEM photograph for the single sheet after 800 °C thermal reduction (under 20% H_2/Ar), and the large sheet breaks into small domains after the high-temperature reduction process. These domains are still well-connected after high-temperature reduction, which is promising for large-size and ultrathin transparent electrodes.

Once the sonication time is increased to 2 h, the GO sheets obtained typically range from 50 to 100 μm in lateral size as shown in the optical micrograph (Figure 1c). More optical images of large GO sheets are provided in the Supporting Information, Figure S3. The size of the obtained GO sheets becomes smaller than 10 μm in lateral size if the sonication time is further increased to 6 h.

The GO sheets after chemical or thermal reduction have been demonstrated to be used as conducting thin-film electrodes.[14−16,34,35] Here, we show that it is

(33) Cote, L. J.; Kim, F.; Huang, J. *J. Am. Chem. Soc.* **2009**, *131*, 1043.
(34) Si, Y.; Samulski, E. T. *Nano Lett.* **2008**, *8*, 1679–1682.
(35) Pang, S.; Tsao, H. N.; Feng, X.; Mullen, K. *Adv. Mater.* **2009**, *21*, 1.

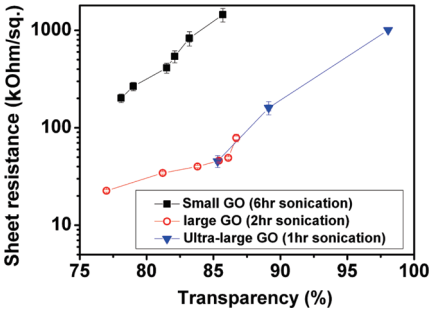

Figure 2. Sheet resistance as function of transparency (T% at 550 nm) for the electrodes prepared from ultra-large-, large-, and smal-size reduced GO sheets after 800 °C thermal annealing (20% H_2 in Ar).

Table 1. Comparison of Ultrathin Electrodes Prepare from Various Reduced GO Sheets

sample ID	process	transparency (% @550 nm)	resistance (KOhm/□)
1	20%H_2 800 °C, 2h	98.0	1005
2	20%H_2 900 °C, 2h	98.1	413
3	20%/H_2 1000 °C, 2h	98.0	188
4[a]	1100 °C vacuum	95.0	500

[a] From ref 36.

advantageous to use larger size of GO sheets for conducting thin-film electrodes. The GO solution was air-sprayed or dip-coated on substrates and reduced with 800 °C annealing in 20% H_2/Ar for 2 h. Figure 2 shows that the sheet resistance of the electrodes prepared from the small-size GO sheets (typical lateral size ~1−5 μm; with 6 h sonication) was significantly higher than those prepared from large size GO (typical size 20−100 μm; with 2 h sonication) or those from ultralarge GO (typical size approximately millimter; with 1 h sonication). Only ultralarge monolayered GO sheets are able to form a conductive electrode with 98% transparency (2% absorption is known to be attributed to the absorption from monolayered graphene). Two other types of GO films (large and small) are not able to form a conductive electrode with such a high transparency (monolayered film) because the stacking of GO sheets, which reduces the transparency, is necessary to form a conduction path. Table 1 shows the annealing temperature effect on the resistance of the ultralarge GO transparent electrodes, where its sheet resistance decreases from ~1000 KΩ/□ (800 °C annealing) to ~188 KΩ/□ (1000 °C annealing). It is noted that the sheet resistance for electrodes made from monolayered ultralarge GO films reduced at 1000 °C (188 KΩ/□) is already lower than (or comparable with) the 500 KΩ/□ ($T \approx 95\%$;) obtained from a thicker film under vacuum annealing at a higher temperature (1100 °C).[36] Note that the sheet resistances that we have achieved, although lower than in previous work, are still too high for practical applications. Therefore, further investigations would be necessary to lower the resistance even more substantially.

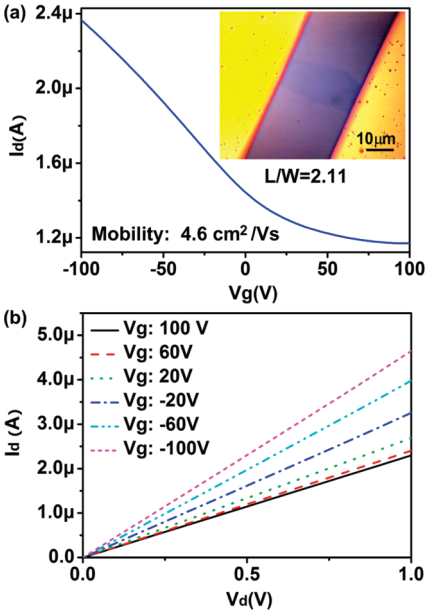

Figure 3. (a) Optical image and transfer curve (I_d-V_g), (b) drain current vs drain voltage for the transistor device made from a single-layer reduced GO sheet under difference applied gate voltages.

The modified Hummers' method allows us to obtain high-yield, ultralarge, and single-layer GO sheets, which can be further converted to large-size reduced GO monolayers by chemical or thermal reduction. Therefore, electronic devices can be easily fabricated without using elaborate electron-beam lithographic techniques. In this study, hydrazine reduction was performed with and without subsequent thermal annealing (400 and 800 °C in 20% H_2/Ar) to optimize the electrical properties of the single-layer reduced GO sheets. Bottom-gate operated transistors based on these reduced GO sheets were fabricated by evaporating Au electrodes directly on top of the GO sheets that were previously deposited on SiO_2/Si substrates. The transfer curves were measured to evaluate the efficiency of the GO reduction processes. Figure 3a demonstrates the typical transfer characteristics for a single-layer GO sheet after hydrazine reduction and 800 °C thermal annealing. Figure 3b shows the drain current (I_d) vs drain voltage (V_d) characteristics for this device and its effective field effect hole mobility extracted from Figure 3a is ~4.6 cm^2/(V s). Only the selected GO sheets with regular shapes and suitable size (~10 μm × 30 μm) were used for the transistor measurements in order to extract the effective field effective mobility of holes. The field-effect mobility of holes was extracted based on the slope $\Delta I_d/\Delta V_g$ fitted to the linear regime of the transfer curves using the equation $\mu = (L/WC_{ox}V_d)(\Delta I_d/\Delta V_g)$, where L and W are the channel length and width, and C_{ox} the gate capacitance. Figure 4 summarizes the statistical mobility values extracted from the transistor devices made from single-layer GO sheets reduced by three processes: (1) hydrazine reduction, (2) hydrazine reduction + 400 °C annealing (20% H_2/Ar), and (3) hydrazine reduction + 800 °C annealing (20% H_2/Ar). It is observed that the mobility of the GO reduced by hydrazine reduction is at ~0.1 cm^2/(V s), consistent with

(36) Wu, J.; Becerril, H. A.; Bao, Z.; Liu, Z.; Chen, Y.; Peumans, P. *Appl. Phys. Lett.* **2008**, *92*, 263302.

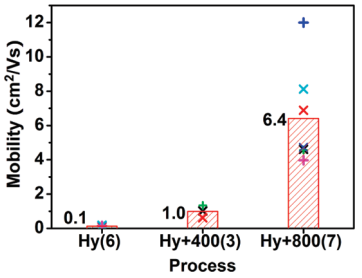

Figure 4. Statistical mobility values extracted from the transistor devices made from single-layer GO sheets reduced by three processes: (1) hydrazine reduction, (2) hydrazine reduction + 400 °C annealing (20% H_2/Ar), and (3) hydrazine reduction + 800 °C annealing (20% H_2/Ar). The number in the parentheses indicates the number of devices tested.

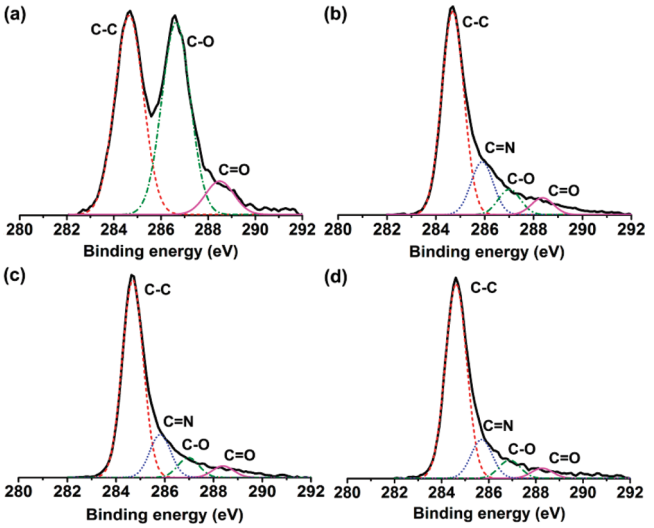

Figure 5. XPS spectra and identified binding energies for (a) as-prepared GO sheets, and the GO sheets after (b) hydrazine reduction, (c) hydrazine reduction + 400 °C annealing (20% H_2/Ar), and (d) hydrazine reduction + 800 °C annealing (20% H_2/Ar).

previous reports. Thermal reduction at 400 °C significantly improves the mobility by around 10 times (to ~1.0 cm^2/(V s)). High-temperature (800 °C) annealing allows us to consistently obtain devices with high mobility ranged from 4 to 12 cm^2/(V s). Small hysteretic responses exist in the transfer curves of the devices (see the Supporting Information, Figure S4 for details); however, the mobility extracted from the forward V_g scan is not significantly different from that obtained in the reverse scan (as shown in Table 2). The large variation of the device mobility may be related to the differences of the size and shape of the GO sheets. In spite of the relatively good mobility obtained for reduced GO sheets compared with other organic materials, several issues still need to be overcome before practical uses, including high threshold voltage, low on−off ratio, and nonsaturated output curves. We notice that in an earlier report the hole mobility for the GO prepared from conventional Hummers' method was estimated to be ~850 cm^2/(V s) (using different method to extract the mobility). Meanwhile, the epitaxial graphene (EG) was used as the metal contacts to reduced the

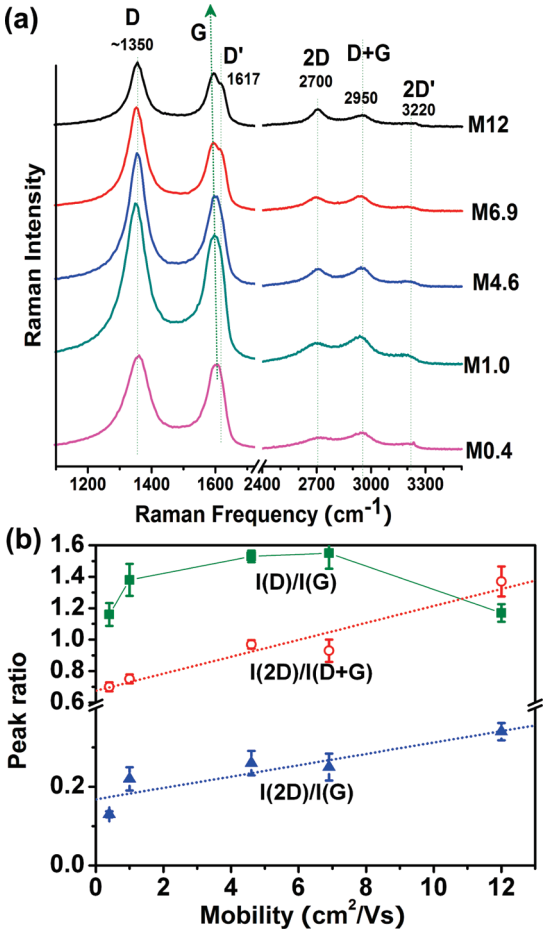

Figure 6. (a) Raman spectra for 5 selected transistor devices with various values of effective mobility. The labels M0.4, M1.0, M4.6, M6.9, and M12 represent the devices with mobility 0.4, 1.0, 4.6, 6.9, and 12 cm^2/(V s), respectively. (b) Various ratios for the integrated peak area for D, G, 2D, and D+G bands.

contact barrier between GO and EG.[37] It is believed that the metal−GO junctions also affect the effective field effect mobility, which warrants further investigations.

Figure 5 shows the C1s X-ray photoemission spectroscopy (XPS) results for the as-prepared GO sheets and those after various reduction processes as described in Figure 4. At least three components C−C (at 284.6 eV), C−O (at 286.6 eV), and C═O (at 288.5 eV) are present in GO sheets.[14,16,27,38] After hydrazine reduction, the peak intensities for C−O and C═O peaks are much smaller than those in GO and an additional peak corresponding to the binding energy of C−N appears, consistent with previous reports.[14,16] Upon subsequent thermal treatments, the peak intensities for the peaks associated with C−N, C−O, and C═O slightly decrease. We notice that the change of the peak intensities for C−N, C−O, and C═O from Figure 5c (hydrazine reduction + 400 °C annealing) to Figure 5d (hydrazine reduction + 800 °C annealing) is not as obvious as the corresponding change in mobility (as summarized in Figure 4). This suggests that the removal of functional groups or heteroatoms

(37) Wu, X.; Sprinkle, M.; Li, X.; Ming, F.; Berger, C.; de Heer, W. A. *Phys. Rev. Lett.* **2007**, *101*, 026801.

(38) Watcharotone, S.; Dikin, D. A.; Stankovich, S.; Piner, R.; Jung, I.; Dommett, G. H. B.; Evmenenko, G.; Wu, S. E.; Chen, S. F.; Liu, C. P.; Nguyen, S. T.; Ruoff, R. S. *Nano Lett.* **2007**, *7*, 1888–1892.

Table 2. Raman Characteristics for Five Selected Transistors Made from Reduced GO

	mobility (cm^2/(V s))					
	forward scan	reverse scan	Pos(G) cm^{-1}	I(D)/I(G)	I(2D)/I(G)	I(2D)/I(D+G)
M12	12.01	12.35	1586.7	1.17	0.34	1.37
M6.9	6.95	6.89	1584.7	1.55	0.25	0.93
M4.6	4.56	4.62	1597.0	1.53	0.26	0.97
M1.0	0.99	1.05	1596.9	1.38	0.22	0.75
M0.4	0.40	0.46	1596.6	1.16	0.13	0.70

(O or N) in reduced GO sheets may not be the only explanation for their mobility enhancements.

To correlate the electrical properties of the single-layer GO sheets with their structural changes, confocal Raman spectroscopy was adopted to directly characterize the reduced GO sheets on transistor devices. Figure 6a shows the Raman spectra for 5 selected transistor devices with various values in effective mobility. The labels M0.4, M1.0, M4.6, M6.9, and M12 represent the devices with mobility 0.4, 1.0, 4.6, 6.9, and 12 cm^2/(V s), respectively. The well-known G peak (at ~1585 cm^{-1}) is characteristic for sp^2-hybridized carbon−carbon bonds in graphene.[39−41] The second prominent peak, 2D band located at ~2700 cm^{-1}, is originated from a double-resonance process.[42−45] D band (~1350 cm^{-1}) exhibits as half of the 2D band energy. An increase in the number of defects would result in an increase of the *D* peak intensity and a concomitant drop in the intensity of the 2*D* peak.[42] In addition, the D′ (~1620 cm^{-1}) peak is also a lattice disorder induced band from the double resonance Raman process due to intravalley scattering.[46,47] It is clearly seen from Figure 6a that G band is shifted to a lower energy with the mobility of the reduced GO sheets and therefore the D′ band becomes more easily deconvoluted. Peak fittings were performed to extract the peak intensity and area for all spectra and the results were tabulated in Table 2. It is noted that the peak area ratio between 2D and G bands, I(2D)/I(G), of the reduced GO sheets increases with their mobility. Both the G band downshift and increase of I(2D)/I(G) ratio can be attributed to either (1) dedoping of p-typed carriers in graphene[13,48−49] or (2) recovering of sp^2 C=C bonds (graphitization) in graphitic structures.[42] However, it is notable that the G band frequency of the GO is at around 1596 cm^{-1}, suggesting that the structure of the GO is more like highly amorphized with isolated double bonds.[46] Therefore, the graphitization appears to be a more appropriate explanation for the increase of I(2D)/I(G).

The I(D)/I(G) ratio has been used to indicate the average size of C sp^2 domain.[27,47,50] Recently, Paredes et al. has argued that the I(D)/I(G) ratio may not be used as an indicator of structural order between amorphous and graphitic materials.[51] Figure 6b shows that the I(D)/I(G) increases with the device mobility at low mobility regime (from 0.1 to 6.9 cm^2/(V s)) and it is attributed to that the GO sheets are changing from amorphized states to more graphitic structures with significant amounts of defects.[51] In fact, at a low-mobility regime, the D band arises from the aromatic rings in the graphitic structures, and therefore the intensity of the D band can be used to indicate the richness of the 6-fold aromatic ring.[44] The G band is caused by in-plane bond stretching of pairs of sp^2 C atoms, and it occurs at all sp^2 sites. Therefore, at a low-mobility regime, the increase in the I(D)/I(G) ratio is actually well-associated with the increase in 6-fold aromatic ring. Similarly, the I(2D)/I(G) also increases with mobility at a low-mobility regime. By contrast, at a higher-mobility regime, where the structure of reduced GO is closer to the graphene structure, the I(D)/I(G) decreases with decreasing disorder in graphitic structures. Thus, I(D)/I(G) decrease with the increasing mobility. On the basis of Figure 6b, it is suggested that the I(2D)/I(G) ratio is a good indicator to correlate the electrical properties with their structures. Moreover, Figure 6b shows that the ratio between the 2D and D+G (~2950 cm^{-1}) peak areas, I(2D)/I(D+G), may also be used as an indicator.

Conclusions

Because of the great promise of graphene oxide sheets in solution-processable electronic applications the research efforts in increasing their lateral size and promoting their electrical properties are crucial. Here, we have demonstrated that the ultralarge GO monolayers (up to several mm in lateral size) can be obtained by a modified Hummers' method. The introduction of sonication step in the modified Hummers' method is able to better adjust the size of the obtained GO sheets. With high temperature

(39) Gupta, A.; Chen, G.; Joshi, P.; Tadigadapa, S.; Eklund, P. C. *Nano Lett*. **2006**, *6*, 2667–2673.
(40) Ferrari, A. C.; Meyer, J. C.; Scardaci, V.; Casiraghi, C.; Lazzeri, M.; Mauri, F.; Piscanec, S.; Jiang, D.; Novoselov, K. S.; Roth, S.; Geim, A. K. *Phys. Rev. Lett*. **2006**, *97*, 187401.
(41) Graf, D.; Molitor, F.; Ensslin, K.; Stampfer, C.; Jungen, A.; Hierold, C.; Wirtz, L. *Nano Lett*. **2007**, *7*, 238–242.
(42) Krauss, B.; Lohmann, T.; Chae, D. H.; Haluska, M.; von Klitzing, K.; Smet, J. H. *Phys. Rev. B* **2009**, *79*, 165428.
(43) Pimenta, P. A.; Dresselhaus, G.; Dresselhaus, M. S.; Cancado, L. G.; Jorio, A.; Saito, R. *Phys. Chem. Chem. Phys*. **2007**, *9*, 1276–1291.
(44) Ferrari, A. C.; Robertson, J. *Phys. Rev. B* **2000**, *61*, 14095–14107.
(45) Ferrari, A. C. *Solid State Commun*. **2007**, *143*, 47–57.
(46) Kudin, K. N.; Ozbas, B.; Schniepp, H. C.; Prud'homme, R. K.; Aksay, I. A.; Car, R. *Nano Lett*. **2008**, *8*, 36–41.
(47) Saito, R.; Jorio, A.; Souza, A. G.; Dresselhaus, G.; Dresselhaus, M. S.; Pimenta, P. A. *Phys. Rev. Lett*. **2002**, *88*, 027401.
(48) Dong, X. C.; Fu, D. L.; Fang, W.; Shi, Y. M.; Chen, P.; Li, L. J. *Small* **2009**, *5*, 1422–1426.
(49) Yan, J.; Zhang, Y. B.; Kim, P.; Pinczuk, A. *Phys. Rev. Lett*. **2007**, *98*, 166802.
(50) Park, S.; An, J. H.; Piner, R. D.; Jung, I.; Yang, D. X.; Velamakanni, A.; Nguyen, S. T.; Ruoff, R. S. *Chem. Mater*. **2008**, *20*, 6592–6594.
(51) Paredes, J. I.; Villar-Rodil, S.; Solis-Fernandez, P.; Martinez-Alonso, A.; Tascon, J. M. D. *Langmuir* **2009**, *25*, 5957–5968.

reduction, these GO sheets are converted to graphitic structures and exhibit relatively high mobility (4−12 $cm^2/(V\ s)$). Note that the sheet resistance we have achieved using ultralarge GO sheets (~188 KOhm/□ with 98% transparency), although lower than in previous work, is still too high for practical applications. Therefore, further investigations would be necessary to lower the resistance even more substantially. Raman spectroscopic studies show that the structure of the GO sheets is converted from amorphized to more graphitic states and the ratio $I(2D)/I(G)$ is better correlated the hole mobility of the GO sheets.

Acknowledgment. This research was mainly supported by Nanyang Technological University, Singapore. We also acknowledge financial support from the National Research Foundation Singapore (NRF- CRP2−2007−02).

Supporting Information Available: AFM, SEM and optical micrographs, and transfer characteristics for the devices (PDF). This material is available free of charge via the Internet at http://pubs.acs.org/.